DISCLAIMER

This report was prepared as an account of work sponsored by an agency of the United States Government. Neither the United States Government nor any agency thereof, nor any of their employees, makes any warranty, express or implied, or assumes any legal liability or responsibility for the accuracy, completeness, or usefulness of any information, apparatus, product, or process disclosed, or represents that its use would not infringe privately owned rights. Reference herein to any specific commercial product, process, or service by trade name, trademark, manufacturer, or otherwise does not necessarily constitute or imply its endorsement, recommendation, or favoring by the United States Government or any agency thereof. The views and opinions of authors expressed herein do not necessarily state or reflect those of the United States Government or any agency thereof. Reference herein to any social initiative (including but not limited to Diversity, Equity, and Inclusion (DEI); Community Benefits Plans (CBP); Justice 40; etc.) is made by the Author independent of any current requirement by the United States Government and does not constitute or imply endorsement, recommendation, or support by the United States Government or any agency thereof.

Pacific Northwest
NATIONAL LABORATORY

PNNL-30456

Iodine Effects on Medical Isotope Producer Delay & Guard Bed Temperature and Performance in Support of NA-23 Program

September 2020

David Stephenson
Paul Humble
Andrew Ritzmann
Praveen Thallapally
James C. Hayes
Katie A. Wagner

U.S. DEPARTMENT OF ENERGY

Prepared for the U.S. Department of Energy
under Contract DE-AC05-76RL01830

DISCLAIMER

PACIFIC NORTHWEST NATIONAL LABORATORY
operated by
BATTELLE
for the
UNITED STATES DEPARTMENT OF ENERGY
under Contract DE-AC05-76RL01830

Printed in the United States of America

Available to DOE and DOE contractors from
the Office of Scientific and Technical Information,
P.O. Box 62, Oak Ridge, TN 37831-0062
www.osti.gov
ph: (865) 576-8401
fox: (865) 576-5728
email: reports@osti.gov

Available to the public from the National Technical Information Service
5301 Shawnee Rd., Alexandria, VA 22312
ph: (800) 553-NTIS (6847)
or (703) 605-6000
email: info@ntis.gov

Online ordering: http://www.ntis.gov

PNNL-30456

Iodine Effects on Medical Isotope Producer Delay & Guard Bed Temperature and Performance in Support of NA-23 Program

September 2020

David Stephenson
Paul Humble
Andrew Ritzmann
Praveen Thallapally
James C. Hayes
Katie A. Wagner

Prepared for
the U.S. Department of Energy
under Contract DE-AC05-76RL01830

Pacific Northwest National Laboratory
Richland, Washington 99354

Summary

In support of NA-23's objective to accelerate the establishment of a reliable commercial United States (U.S.) domestic supply of ^{99}Mo produced without the use of highly enriched uranium (HEU), the Pacific Northwest National Laboratory (PNNL) was tasked with modeling the performance of activated carbon delay and guard beds that may be typical for non-HEU ^{99}Mo production processes. The specific tasks accomplished by PNNL included calculations of long-term effects of iodine on delay bed performance and development of a finite element simulation to better understand delay bed performance under various scenarios specifically with radioxenon and radioiodine decay heating of the delay beds. The main issue of interest in this study is understanding the effect of iodine on the abatement performance of the beds if iodine is not sufficiently removed from gases prior to reaching the delay beds. Finite element simulations of delay bed performance were developed using COMSOL Multiphysics® Software. These simulations are based on partial differential equations that describe xenon and iodine adsorption, heat transfer and decay of radioxenon and radioiodine isotopes. Heat transfer in the activated carbon beds is simulated with a heat source tied to the decay of radioactive xenon and iodine species. These simulations were used to investigate delay bed temperature and hold up time using radioxenon and radioiodine activities and flowrates expected from a non-HEU production process. A bounding case scenario was simulated, where all the iodine was released into the delay beds due to insufficient guarding of the delay beds. In addition, preliminary investigations of the guard beds were conducted.

Acronyms and Abbreviations

HEU Highly enriched uranium
LEU Low enriched uranium
PNNL Pacific Northwest National Laboratory

Nomenclature

c	concentration (mol/m^3)
C_p	heat capacity (J/kg*K)
d_p	particle diameter (m)
h	heat transfer coefficient (W/m^2*K)
k	kinetic (rate) constant (1/s)
K	thermal conductivity (W/m*K)
L	length of packed bed (m)
Q	heat of adsorption (J/mol)
Q'	energy of radioactive decay (J/mol)
r	radius of packed bed (m)
R	ideal gas constant (J/mol*K)
S	specific surface area (1/m)
t	time (s)
T	temperature (K)
V	gas flow rate (m^3/s)

Greek

ε	porosity of the activated carbon bed
λ	radioactive decay constant (1/s)
κ	permeability (m^{-2})
μ	viscosity (Pa·s)
ρ_g	gas density (kg/m^3)
ρ_b	bulk density of adsorbent (kg/m^3)

Subscript

i	species/isotope
b	property of the packed bed
g	property of air

Superscript

* equilibrium value

Contents

Figures

Tables

1.0 Introduction

Production of ^{99}Mo from fission of low enriched uranium (LEU) or highly enriched uranium (HEU) creates radioxenon and radioiodine as byproducts that can exceed regulatory levels for health and safety if released to the environment. To reduce radioxenon and radioiodine emission levels, producers have incorporated several engineered methods to capture or delay the release of radioxenon, allowing the short-lived isotopes to decay (e.g., 5.2-day half-life for ^{133}Xe). These methods include, guard beds, adsorption delay beds and holding tanks. In most cases, adsorption delay beds are large and require significant radiation shielding to minimize exposure to workers and the public. There is a drive to better understand how to minimize the size of the delay beds while maintaining all safety and abatement objectives. The Pacific Northwest National Laboratory (PNNL) has a 25-year history of developing new materials and systems that collect and measure radioxenons in atmospheric samples. In addition, PNNL has established expertise in measuring adsorbent properties and has developed methods to account for the heat of decay in xenon adsorption models that result from trapped radioactive noble gas species, which are similar to those models used for radioxenon abatement in the nuclear industry.

The goal of this research is to improve radioiodine abatement technologies for medical isotope producers. In this study, a finite element simulation was developed to better understand delay bed performance under various scenarios specifically with radioxenon and radioiodine decay heating of the delay beds. Breakthrough calculations were developed for modeling delay bed performance of potential adsorbents, which include simulations of heat effects due to radioactive decay. The main issue of interest in this study is understanding the effect of iodine on the abatement performance of the delay beds if iodine is not sufficiently abated from gases prior to reaching the delay beds.

Initial investigations of the guard bed were conducted and are presented in Appendix A.

2.0 Delay Bed Deactivation Mechanisms

In medical isotope production, delay beds are designed to reduce the activity of radioxenon released to the environment to acceptable levels. Iodine that adsorbs irreversibility on activated carbon will take up sorption sites, thereby decreasing the available bed capacity for xenon abatement. Bhatia [1] suggests that 57% of the iodine adsorbs irreversibly on activated carbon at ambient temperature. For this effort we assumed delay beds that have a 90 in. diameter and 960 in. of total length. Given the large size and the amount of possible iodine that can be adsorbed in the delay beds (71 tons of activated carbon with 107 tons of possible irreversible iodine uptake based on Bhatia's work), if a medical isotope producer expects approximately 5 g of iodine to be produced annually it is unlikely that the delay bed's capacity would be significantly reduced.

Delay beds are expected to operate for 30+ years, any decreases in bed capacity from irreversible adsorption of iodine has the potential to reduce the life expectancy of the delay beds. To reduce the likelihood of this occurring, medical isotope producers may include a guard bed in the process flow prior to the delay bed(s). Given an estimated of 5 g of iodine being produced per year (2,000 Ci of ^{133}I per day), different estimates of delay bed capacity decrease were estimated. The estimates consider guard bed performance ranging from nonexistent 0% to 99.99% effective over a 30-year timeframe. Simulating delay beds that contain 71 tons of coconut shell activated carbon, the capacity change over time are shown in Figure 1.

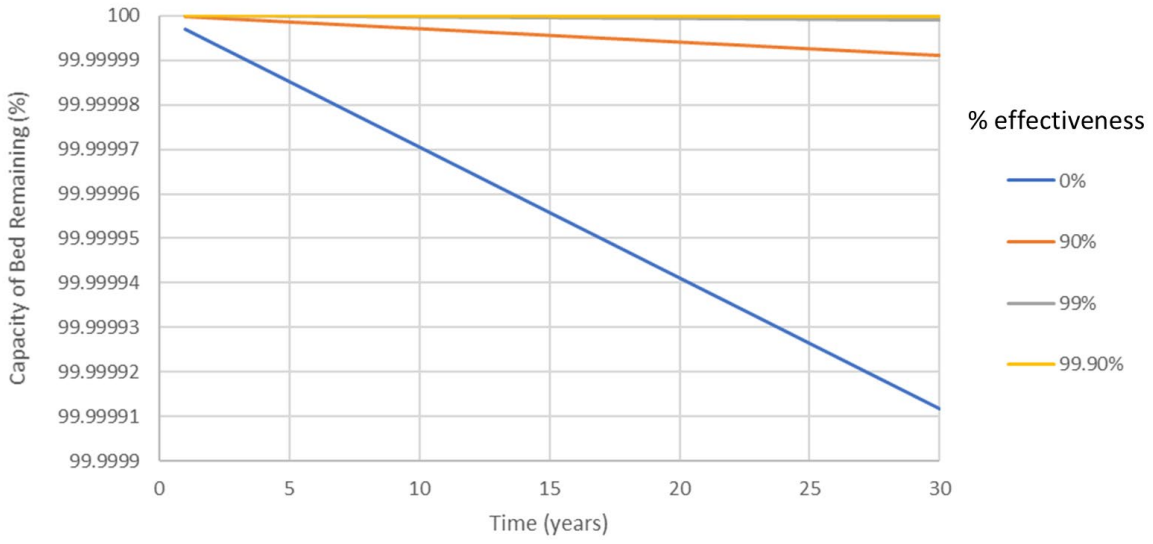

Figure 1. The estimated capacity of delay beds over time for different delay bed performances.

Assuming no guard bed in the process flow and the low estimated amounts of iodine to be released, the capacity of the delay beds is reduced by 0.00009% over a 30-year timeframe (Figure 1). This reduction in delay bed capacity is conservative due to assuming all the iodine produced is stable, while in reality, a mixture of radioactive and stable iodine is produced. Monte Carlo N-Particle Transport Code (MCNP) coupled with Oak Ridge Isotope GENeration (ORIGEN) calculations approximate that only ~1% of the produced iodine to be stable ^{127}I with

the balance being unstable radioiodine species. The radioactive ^{131}I species will decay to ^{131}Xe species which will not irreversibly adsorb. Other species, ^{133}I and ^{135}I, will eventually decay to stable ^{133}Cs and ^{135}Ba which may adsorb strongly, causing delay bed performance degradation. However, due to the small amount of expected ^{133}Cs, ^{135}Ba, and ^{127}I, it is expected that that actual performance reduction may be much lower than what was calculated in Figure 1. While this change in delay bed capacity suggests that guard beds may not be required over the lifetime of the plant, shorter lived iodine species may produce significant amounts of heat. Removing the radioactive iodine species heat with a guard bed will allow for delay beds to operate closer to their expected room temperature performance.

Simple modeling of 71 tons of coconut shell activated carbon in a delay bed would suggest that iodine breakthrough may be on the order of around 1,553 years (0.003% xenon and iodine combined mole fractions). Given that the half-life of the longest iodine species considered in this study is 8 days, it is likely that all iodine would decay to xenon very close to the beginning of the first of the eight delay beds. Such a small distance change in xenon introduction into the delay beds would not likely affect the delay time of the delay beds.

However, simple models do not couple the effects of radioxenon and radioiodine heating on the delay bed performance. In order to couple heating effects to delay bed performance a different more complex model needs to be simulated. A preliminary look at such modeling was performed using finite element software (COMSOL Multiphysics® Software) to model the appropriate coupled equations.

3.0 Adsorption Data from Bhatia Fitted with Assumptions

Three assumptions were made based on insufficient iodine adsorption data on currently available coconut shell activated carbons at the time of this study.

- Assumption 1: Available sites for adsorption of species is ~0.01 mol/g of carbon. This is typical of what is seen in literature [1, 2] and experimental data collected at PNNL for nitrogen, xenon, and iodine. This equates to 2.6 grams of iodine per gram of carbon.
- Assumption 2: Isotherm data from Bhatia [1] from their tested carbon was scaled so that it matched expected available adsorption sites for Nucon's activated carbons and other currently available activated coconut shell carbon. This added 26% to the adsorption capacity of the carbon in comparison to what was reported by Bhatia [1].
- Assumption 3: Estimated adsorption and desorption rates of iodine on carbon were performed using iodine adsorption and desorption data from Bhatia [1]. Due to the small amount of stable ^{127}I, the irreversible adsorption of some of the stable ^{127}I is ignored in simulations by modeling iodine desorption as completely reversable. Modeling desorption processes as reversable is conservative because if some iodine were irreversibly adsorbed then a slower holdup of iodine on the delay beds would be expected.

Based on the above assumptions the Langmuir fits of Bhatia's data are shown in Figure 2.

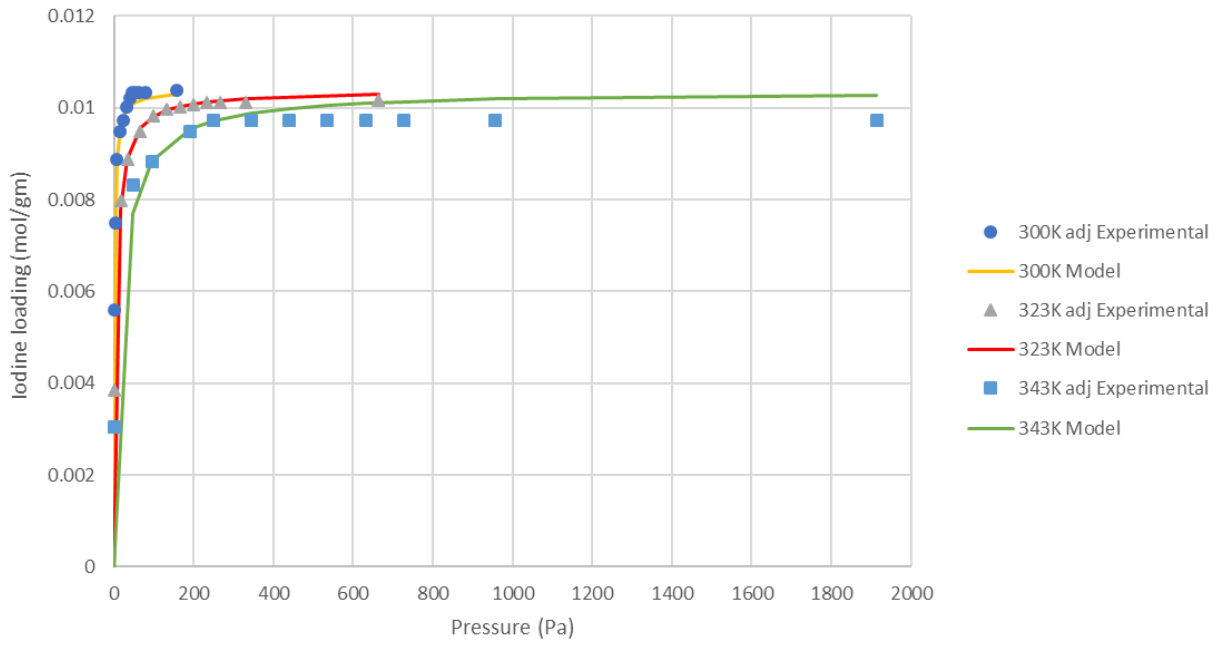

Figure 2. Iodine adsorption data from Bhatia adjusted to have 0.01 mol/g of active sites at 300K. [1] Solid lines show the Langmuir isotherm fits. The resulting Langmuir parameters are listed in Table 1.

Estimating the forward and reverse kinetic rates were also performed using adsorption and desorption data from Bhatia. [1] Fitted data are shown in Figure 3 and Figure 4.

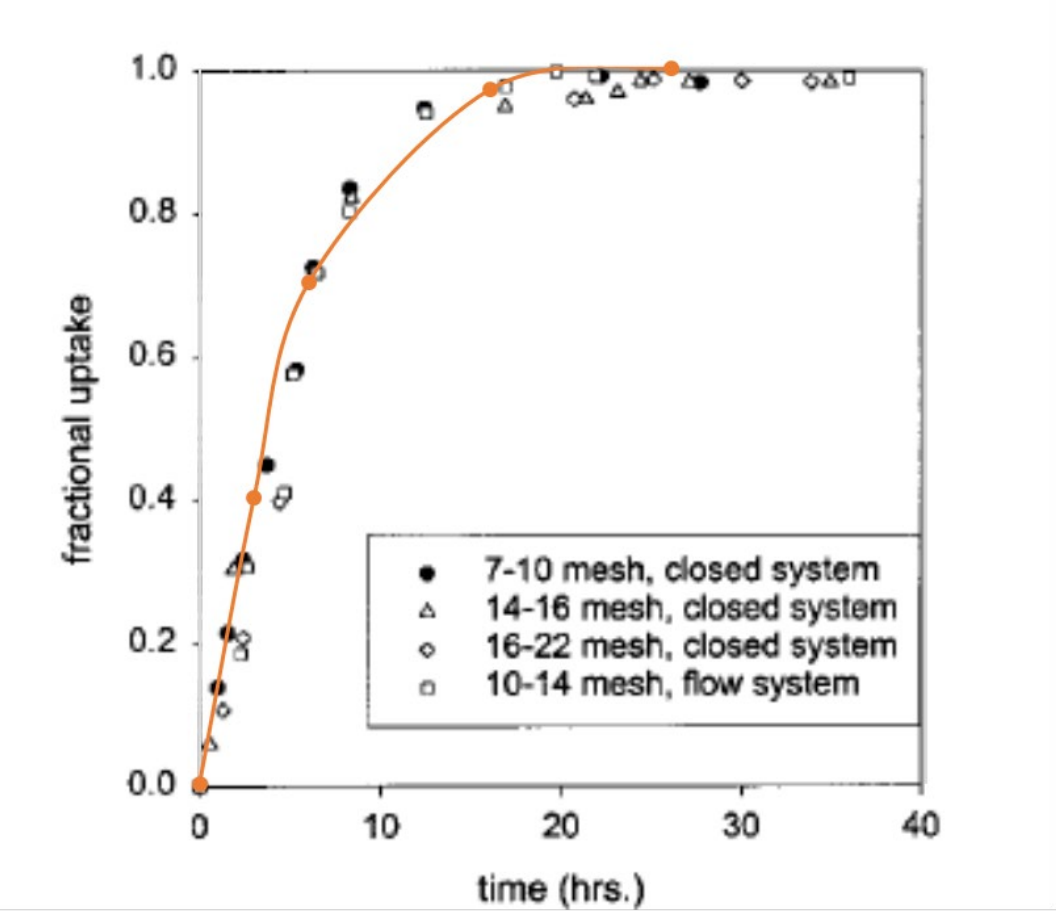

Figure 3. Fitted data from Bhatia [1] to estimate adsorption kinetics of iodine.

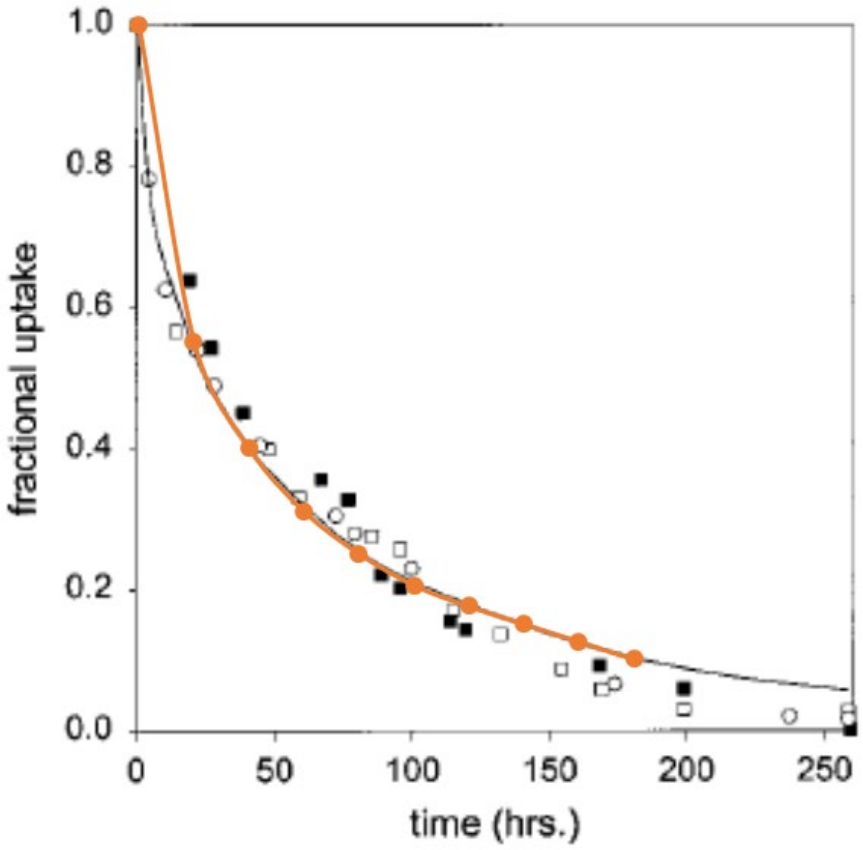

Figure 4. Fitted data from Bhatia [1] to estimate desorption kinetics of iodine.

An adsorption uptake rate constant of 2.97 1/s was roughly estimated for where the iodine partial pressure is known (Figure 3). Similarly, a desorption rate constant of 0.61 1/s was estimated (Figure 4). Langmuir isotherm fits of Bhatia scaled data from Figure 2 are in Table 1 (see Section 5.1), as well as other model parameters used in the finite element simulations and ideal calculations of adsorbent bed abatement.

4.0 Model Equations

COMSOL simulations can couple adsorption of xenon and iodine species and the effects of their radioactive decay heating on bed performance. In this report the gas species modeled included ^{131}Xe, ^{133}Xe, ^{135}Xe, ^{131}I, ^{133}I, ^{135}I, and N_2. In addition, the radioactive decay heat of all radioactive species was modeled along with their decay into other gas species. A worst-case approach was modeled where only iodine species were introduced into the bed which then decayed into their respective xenon species. This is considered the worst case because there is no abatement by a guard bed or delay time from dissolution processes of these species before introduction into the delay bed. The purpose of this simulation is to determine the maximum expected heating of the delay beds and the resulting temperature profile.

4.1 Model Assumptions

The xenon abatement system used as a basis for these COMSOL simulations contains large room temperature vessels filled with coconut shell activated carbon. The model assumes that the off gas from the medical isotope facility has been stripped of acid vapors and iodine and has a relative humidity of less than 40%. The off-gas stream is expected to have the same major components as air (*i.e.*, nitrogen, oxygen, and argon).

The following assumptions were used in deriving the partial differential equations governing delay bed performance:

- The gas phase behaves ideally (Darcy's flow).
- Plugs flow through the packed bed.
- Thin-film mass transfer resistance is negligible.
- Gravitational effects are neglected.

4.2 Ideal Calculations

Idealized calculations for iodine breakthrough were performed with a competitive Langmuir adsorption isotherm approach (N_2, xenon, and iodine) to determine the expected ideal hold up times of the delay beds. These calculations do not include dispersion or heating, so they assume that breakthrough occurs when the bed is saturated with respect to the inlet gas stream.

4.3 Gas Transport

Flow through a porous bed is assumed to follow Darcy's law as given in Equation 1 where P is the pressure, c_j is the gas phase concentration of species j, ε is the bed porosity, κ is the permeability of the solid phase, μ is the gas viscosity, R is the ideal gas constant, and T is the temperature. The summation of concentrations in Equation 1 includes all species in the gas phase.

$$q_{Darcy} = -\frac{\kappa}{\mu}\nabla P = -\frac{\kappa RT}{\mu}\nabla\left(\sum_j c_j\right) \quad (1)$$

The gas phase mass balance for each species using Darcy's law and including gas diffusion is given in Equation 2 [3] where λ_i is radioactive decay constant for species I, $D_{i,gas}$ is an effective diffusion coefficient that accounts for all axial dispersion effects, κ was estimated using the empirical equation developed by Rumpf and Gupte. [4]

$$\varepsilon \frac{\partial c_i}{\partial t} + \nabla \cdot \left(-D_{igas} \nabla c_i - c_i \frac{\kappa RT}{\mu} \nabla \left(\sum_{j=1}^{n} c_j \right) \right) = -R_i - \lambda_i c_i \quad (2)$$

4.4 Adsorption

The adsorbed phase mass balance for each species is given in Equation 3 where $c_{i,ad}$ is the concentration of species *i* on the adsorbent R_i is the rate of adsorption.

$$\frac{\partial c_{i,ad}}{\partial t} = R_i - \lambda_i c_{i,ad} \quad (3)$$

The rate of mass transfer between the gas and adsorbed phase is based on a competitive Langmuir adsorption isotherm using the linear driving force approximation (Equation 4).

$$R_i = k_i \cdot \left[\frac{\rho_b N_{io} b_i(T) RT c_i}{1 + \sum_j b_j(T) RT c_j} - c_{i,ad} \right] \quad (4)$$

In equation 4, k_i is the mass-transfer coefficient of species *i*, and $c_{i,ad}$ is the concentration of species *i* in the adsorbed phase, ρ_b is the packed bed density, N_{io} is the saturation capacity of the adsorbent, b_i is the Langmuir constant [5] for species *i* with the adsorbent (obtained using Equation 5), Q_i is the heat of adsorption for species *i* on the adsorbent, and c_i is the concentration of species *i* in the gas phase. This model assumes that the mixture components have the same saturation capacity [6] on a given adsorbent.

$$b_i = b_{io} e^{Q_i / RT} \quad (5)$$

4.5 Heat Transfer

Convection conduction equations were developed to model heat transfer in the delay bed. Separate equations were developed for the gas and adsorbent phases and a heat transfer coefficient was used to model heat transfer between the gas and solid phase. Equation 6 shows the heat transfer equation used for the gas phase. In Equation 6, T_b is the adsorbent temperature, and T_g is the temperature of the gas and, $\overrightarrow{u_g}$ is the velocity of the gas as described by Darcy's flow from Equation 1. In Equation 6 the parameter Cp_g is the heat capacity of the gas, k_g is the thermal conductivity of the gas, $q_{\text{decay,i}}$ is the heat generated by radioactive decay described in Section 4.6, *a* is the specific surface area of the bed, and *h* is heat transfer coefficient for the bed particles. This equation assumes that the gas density is constant (incompressible flow) despite the compressibility of gases. However, this approximation is reasonable in the regime of relatively small temperature changes.

$$\rho_g Cp_g \frac{\partial T_g}{\partial t} + \rho_g Cp_g \overrightarrow{u_g} \nabla T_g + \nabla \cdot \left(-k_g \nabla T_g \right) = q_{\text{decay,i}} + ah\left(T_b - T_g \right) \quad (6)$$

The conduction equation in the adsorption bed for the solid adsorbent phase is given in equation 7. In equation 7, Cp_b is the heat capacity of the bed, and k_b is the thermal conductivity of the bed. The other parameters and variables appearing in this equation are as previously described.

$$\rho_b Cp_b \frac{\partial T_b}{\partial t} + \nabla \cdot (-k_b \nabla T_b) = q_{\text{decay,i}} - ah(T_b - T_g) \quad (7)$$

4.6 Radioactive Decay

Atoms undergoing radioactive decay release copious amounts of energy. It is assumed that the decay energy is the difference between the ground states of the parent and daughter nuclei. ^{133}Xe and ^{135}Xe undergo β decay to form ^{133}Cs and ^{135}Cs, respectively. [7, 8] 427.4 keV (4.12×10^{10} J/mol) and 1165 keV (1.12×10^{11} J/mol) are emitted from the decay of these xenon isotopes respectively. [7, 8] As β decay is the primary mechanism, the decay energy is treated in a local manner to keep the problem tractable. In the same way, ^{131}I, ^{133}I, and ^{135}I undergo β decay as well but their product species are ^{131}Xe, ^{133}Xe, and ^{135}Xe respectively. In the model the iodine decay products are added to their respective product xenon species which then decay in the case of ^{133}Xe and ^{135}Xe. Approximately 970.8 keV (9.37×10^{10} J/mol), 1757 keV (1.70×10^{11} J/mol), and 2627 keV (2.53×10^{11} J/mol) are emitted from the decay of these iodine isotopes respectively. [7-9]

Equation 8 defines the associated heat generation rate ($q_{\text{decay,i}}$) for isotope i where $c_{,\text{i}}$ is the concentration of the species *i* (this is the gas phase concentration for Equation 7, and the adsorbed gas concentration for Equation 8), λ_i is the first order decay constant for the species, and Q'_i is the decay energy in J/mol for the species.

$$q_{\text{decay,i}} = \lambda_\text{i} c_\text{i} Q'_\text{i} \quad (8)$$

The assumption that decay energy deposits locally leads to an overestimation of the radiation heating effects. In fact, advanced radiation transport modeling of a carbon delay bed showed that the total decay heat absorbed in the bed would be less than half of this overall quantity. The heat will also deposit in a more uniform manner than what is simulated from the local assumption. As a result, local regions of higher temperature will arise in the simulations and lead to shorter breakthrough times compared to a model with a full, stochastic treatment of radiation transport.

5.0 Finite Element Simulations

This section presents COMSOL Multiphysics® software simulations to model flow and activity conditions for radioxenon and radioiodine abatement. COMSOL can solve for the coupled systems of partial differential equations as was presented in the prior section using finite element method.

5.1 Simulation Description and Parameters

The inlet and walls of the cylinders were set at 23°C. The primary interest in the simulations were the estimated maximum temperature for the activated carbon delay beds, and the xenon and iodine retention times. Axisymmetric simulations were used to take advantage of the cylindrical bed geometries. Simulation parameters are reported in Table 5.1.

Table 5.1. Model parameters obtained from measurements and literature sources.

Parameter	Value	Parameter	Value
V (23ºC)	0.782 m^3	Q'_{Xe-135}	1.12 × 10^{11} J/mol
L (23ºC)	0.191 m	λ_{I-131} [e,f]	1.00 × 10^{-6} s^{-1}
R (23ºC)	1.143 m	Q'_{I-131} [f]	9.37 × 10^{10} J/mol
ε	0.43	λ_{I-133} [e,f]	9.26 × 10^{-6} s^{-1}
d_p	0.00129 m	Q'_{I-133} [f]	1.70 × 10^{11} J/mol
D_{Xenon}	4.4 × 10^{-6} m^2/s	λ_{I-135} [e,f]	2.93 × 10^{-5} s^{-1}
$C_{p,g}$ (300 K, 1 atm)[a]	1010 J/kg*K	Q'_{I-135} [f]	2.53 × 10^{11} J/mol
ρ_g (300 K, 1 atm)[a]	1.18 kg/m^3	N_{Xeo} [g]	1.04 × 10^{-2} mol/gm
k_g (300 K, 1 atm)[a]	0.0262 W/m*K	Q_{Xe} [g]	21100 J/mol
μ_g (300 K, 1 atm)[a]	1.85 × 10^{-5} Pa*s	b_{Xeo} [g]	9.09 × 10^{-9} 1/Pa
Pr_g (300 K, 1 atm)[a]	0.708	N_{N2o} [h]	1.04 × 10^{-2} mol/gm
k_b [b]	0.20 W/m*K	Q_{N2} [h]	19000 J/mol
h [c]	102 W/m^2*K	b_{No} [h]	2.57× 10^{-10} 1/Pa
$C_{p,b}$ [d]	770 J/kg*K	N_{Io} [i]	1.04 × 10^{-2} mol/gm
λ_{Xe-133} [e,f]	1.53 × 10^{-6} s^{-1}	Q_I [i]	50549 J/mol
Q'_{Xe-133}	4.12 × 10^{10} J/mol	b_{Io} [i]	1.20× 10^{-9} 1/Pa
$\lambda_{^{135}Xe}$ [e,f]	2.11 × 10^{-5} s^{-1}	ρ_b [h]	645 kg/m^3

[a] Ref. [10]
[b] Ref. [11]
[c] Computed from the correlation of Gunn [12]
[d] Ref. [13]
[e] Decay constants are calculated from the half-life ($\lambda_i = \ln(2)/t_{1/2,i}$)
f Refs. [7-9, 14]
[g] Fit from adsorption data
[h] Obtained from measurements on Alamo Water activated carbon
[i] Obtained from fitting S. Bhatia's data adjusted to Alamo Water activated carbon active sites [1]

The flowrate into the delay bed was set at 453 slpm (16 scfm). Due to the model complexity, COMSOL had very long required simulation times. To decrease simulation times, the delay bed simulation was run with only a fraction of 71 tons of activated carbon (0.55 tons in this case). Model complexity was due to having seven gas species, radioxenon decay and heating, the necessary model meshing to provide solution stability, and the addition of different kinetic rate constants for adsorption and desorption for iodine species. The selected model geometry was 7.5 in. in length with a cylinder of 90 in. in diameter. As will be discussed in section 5.2, even with a reduced delay bed size being modeled the numerical complexity was too large to do more than estimate the heating and abatement time solution.

The amount of stable ^{131}Xe was set at 0.003% with 2.02E-7% ^{131}I, 5.00E-8% ^{133}I, and 5.41E-9% ^{135}I, with the balance of the gas composition being nitrogen. Decay heat of iodine was simulated using the total decay energies of the iodine species (Table 5.1). Simulations were run with continuous flow of ^{131}Xe, ^{133}Xe, ^{135}Xe, ^{131}I, ^{133}I, ^{135}I, and N_2, and were run until the temperature and concentration profiles reached steady state (240 days).

5.2 Results

Modeling the inlet as an insulating boundary was considered a worst-case scenario, given the inlet would be expected to provide some cooling due to the inlet basically being a wall. With these model assumptions and conditions max bed temperature was to 23.78°C with an average temperature reaching 23.62°C. Wall boundaries were set equal to 23°C with the inlet and outlet boundaries set to no heat flux (insulation). COMSOL temperature results are shown in Figure 5.

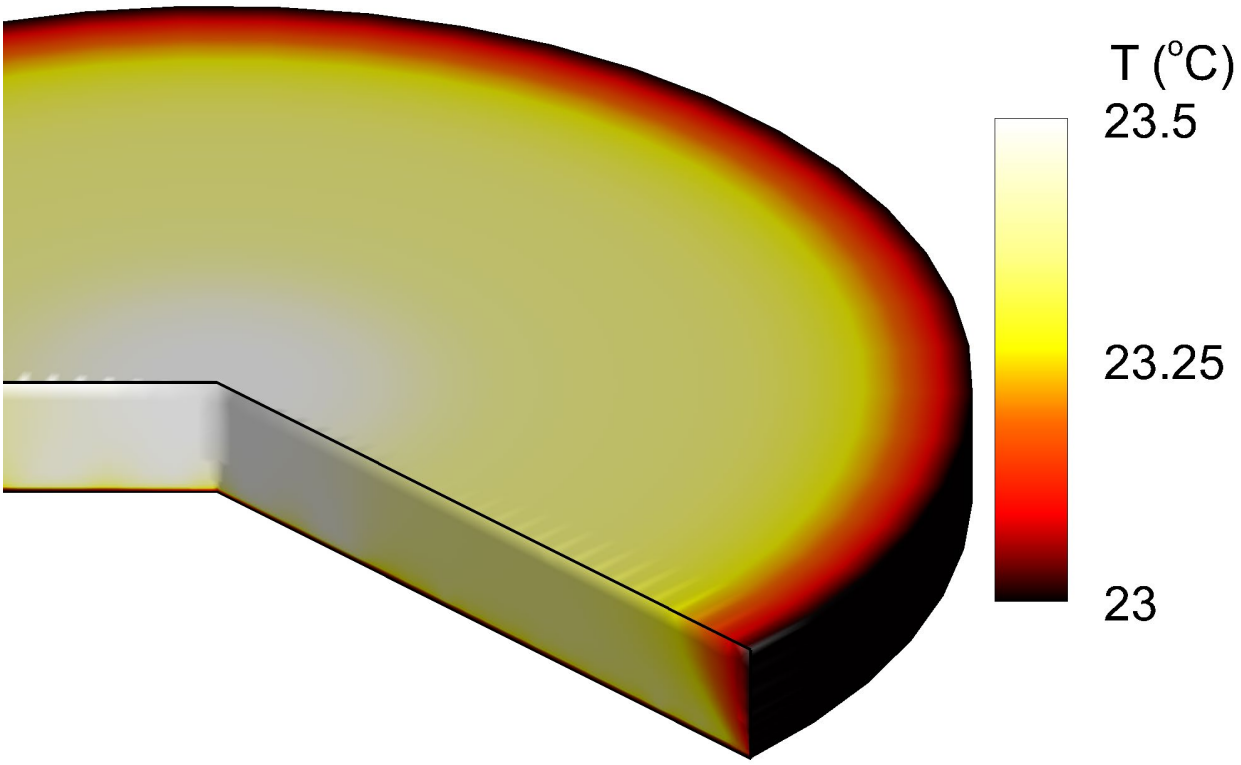

Figure 5. Temperature (°C) results from COMSOL simulation after 240 days of simulation.

One reason for the small change of temperature was the iodine adsorbed rapidly to the activated carbon at the entrance of the bed. Heat released by radioiodine decay into xenon species was removed by the bed wall boundaries. The small temperature rise is likely reasonable due to only around 159.64 watts of heat being produced by nuclear decay heat in the small bed volume being simulated. Figure 6 below shows the distribution ^{131}I in the simulated bed volume after 240 days of simulation.

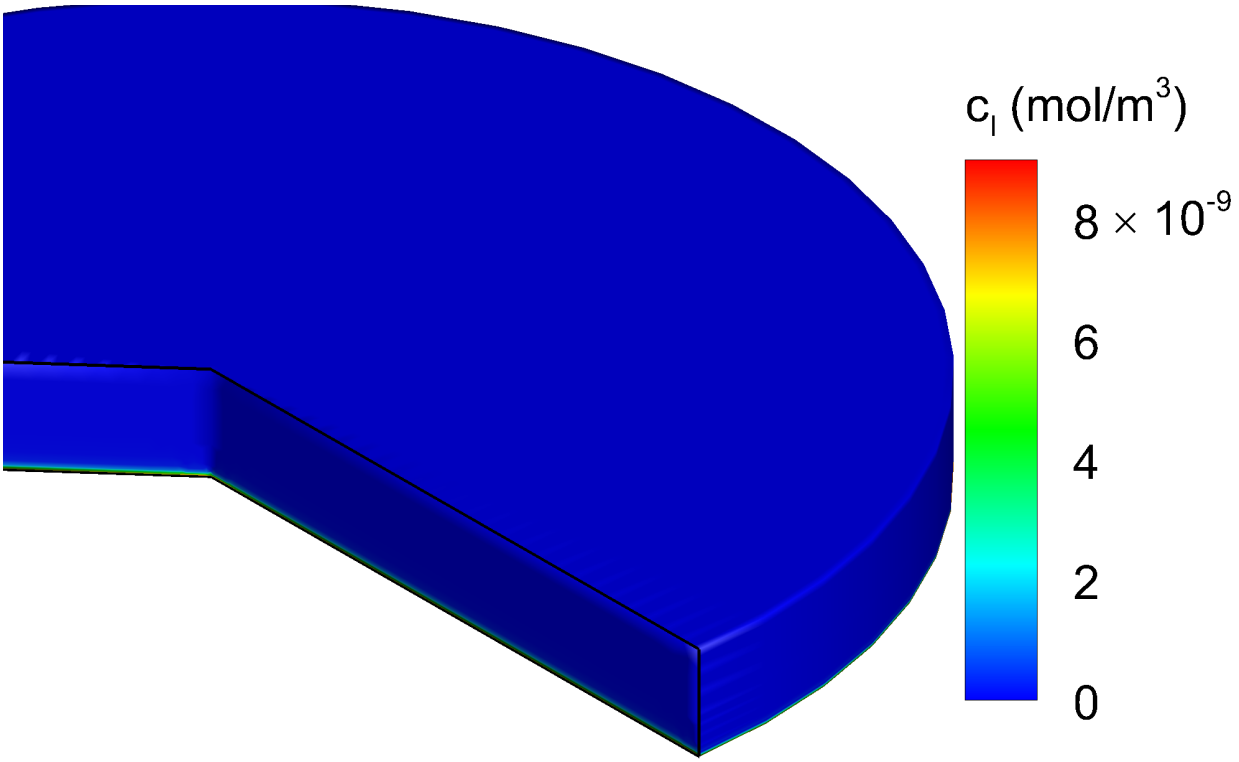

Figure 6. Concentration distribution of ^{131}I (mol/m^3) after 240 days of simulation.

To check the accuracy of the above solutions, another simulation was run with increased model meshing. Increasing meshing caused the model to run 15 days longer, for a solve time of 18 days. The higher meshing solution showed a bed heating of 140.4 watts with a max temperature of 23.41°C and an average temperature of 23.31°C. Bed delay time increased to 107 years which is closer to the ideal 1,556 years for iodine delay. With increased meshing the model solution changed, which indicates that the model likely needs further mesh refinement.

Another check of the accuracy of the simulation was to calculate the maximum amount of heat expected to be released from radioiodine and radioxenon isotopes under the assumption that all are trapped in the delay bed. Using this assumption, it was calculated that a maximum of 88 watts could be expected. It is believed that the extra heat being calculated in the COMSOL is due to numerical error due to not enough model meshing.

However, given that the heating calculated in the current simulations is higher than the maximum heating and the holdup time was shorter than the ideal, the COMSOL simulations can be considered a conservative estimate of radioxenon and radioiodine decay heating on delay bed performance. It is recommended that future work either have increased meshing or simulations of smaller volumes of activated carbons when simulating the full xenon and iodine species sets.

6.0 Conclusions

The series of typical delay beds modeled are estimated to be more than sufficient to capture the radioactive iodine species until they decay (1,556 years, ideal calculations; 54 years, conservative COMSOL calculations). While not enough iodine, cesium, and barium are expected to reach the delay beds to cause a 57% decrease in bed capacity over 30+ years (based on 2000 Ci ^{133}I), iodine and xenon decay heat will likely decrease the expected delay performance. As a result, it is recommended that 90% to 99% of iodine removal be performed prior to the delay beds. However, our models estimate that decay heat from radioiodine will likely not cause a critical failure of delay bed adsorption performance.

7.0 References

1. Bhatia, S.K., F. Liu, and G. Arvind, *Effect of Pore Blockage on Adsorption Isotherms and Dynamics: Anomalous Adsorption of Iodine on Activated Carbon.* Langmuir, 2000. **16**(8): p. 4001-4008.
2. Juhola, A.J., *Iodine adsorption and structure of activated carbons.* Carbon, 1975. **13**(5): p. 437-442.
3. Jin, X., A. Malek, and S. Farooq, *Production of Argon from an Oxygen−Argon Mixture by Pressure Swing Adsorption.* Industrial & Engineering Chemistry Research, 2006. **45**(16): p. 5775-5787.
4. Rumpf, H. and A.R. Gupte, *Influence of Porosity and Particle Size Distribution in Resistance Law of Porous Flow.* Chemie Ingenieur Technik, 1971. **43**(6): p. 367-375.
5. Yang, R.T., *Gas Separation By Adsorption Processes*. Series on Chemical Engineering. Vol. 1. 1997, London: Imperial College Press.
6. Rao, M.B. and S. Sircar, *Thermodynamic Consistency for Binary Gas Adsorption Equilibria.* Langmuir, 1999. **15**(21): p. 7258-7267.
7. Khazov, Y., A. Rodionov, and F.G. Kondev, *Nuclear Data Sheets for A=133.* Nuclear Data Sheets, 2011. **112**(4): p. 855-1113.
8. Singh, B., A.A. Rodionov, and Y.L. Khazov, *Nuclear data sheets for A=135.* Nuclear Data Sheets, 2008. **109**(3): p. 517-698.
9. Khazov, Y., I. Mitropolsky, and A. Rodionov, *Nuclear data sheets for A=131.* Nuclear Data Sheets, 2006. **107**(11): p. 2715-2930.
10. Hilsenrath, J., et al., *Circular of the Bureau of Standards no. 564: Tables of Thermal Properties of Gases Comprising Tables of Thermodynamic and Transport Properties of Air, Argon, Carbon Dioxide, Carbon Monoxide, Hydrogen, Nitrogen, Oxygen, and Steam*. 1955: U.S. Department of Commerce: National Bureau of Standards. 488.
11. Kuwagaki, H., et al., *An improvement of thermal conduction of activated carbon by adding graphite.* Journal of Materials Science, 2003. **38**(15): p. 3279-3284.
12. Gunn, D.J., *Transfer of Heat or Mass to Particles in Fixed and Fluidized-Beds.* International Journal of Heat and Mass Transfer, 1978. **21**(4): p. 467-476.
13. Lutcov, A.I., V.I. Volga, and B.K. Dymov, *Thermal Conductivity, Electric Resistivity and Specific Heat of Dense Graphites.* Carbon, 1970. **8**(6): p. 753-760.
14. Sonzogni, A. *NuDat 2.7*. 2018 [cited 2018 November 14]; Available from: https://www.nndc.bnl.gov/nudat2/.
15. Reyerson, L.H. and A.E. Cameron, *The Sorption of Bromine and Iodine by Activated Charcoal.* The Journal of Physical Chemistry, 1936. **40**(2): p. 233-237.

Appendix A – Preliminary Guard Bed Results

This appendix describes the preliminary results for modeling the radioiodine and radioxenon hold-up time in a modeled guard bed (10 in. diameter by 16 in. length filled with activated coconut shell carbon). The potential pressure losses within the proposed delay bed as a result of modeling in the guard bed are also described here. The assumed process flow includes a guard bed prior to the modeled delay beds to delay radioiodine long enough for it to decay into radioxenon species prior to reaching the delay beds. The guard bed is expected to be operated at ambient temperature. Guard bed modeling uses all the same approximations and model parameters as the delay bed study with the exception of the bed geometry.

A.1 Preliminary Guard Bed Results

For the model, guard bed wall boundaries were set equal to 23°C, similar to the delay beds, with the inlet and outlet boundaries set to no heat flux (insulation). With the same model assumptions and conditions as the delay bed simulations, the max guard bed temperature was to 37.12°C with an average temperature reaching 32.77°C. Modeled temperature results for the guard bed are shown in Figure A.1.

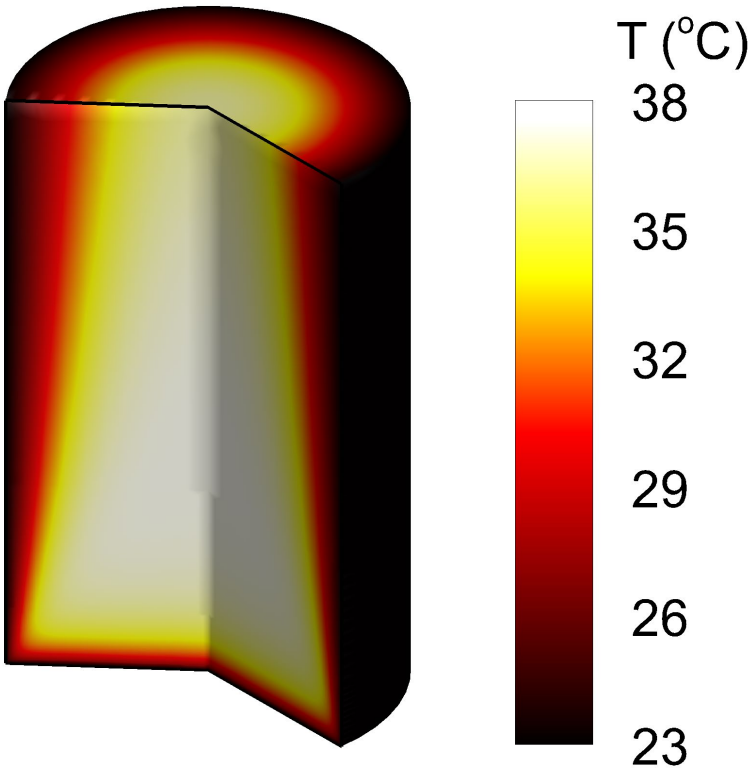

Figure A.1. Temperature (°C) results from COMSOL simulation after 240 days of simulation for the guard bed.

The average modeled power of the guard bed was 89 watts. This indicates that the model has some numerical issues, i.e. greater than the estimated max power of 88 watts. Further

refinement of the model mesh is required for more model accuracy. However, the numerical issues are not anticipated to significantly alter the results of the model.

The overall higher temperatures of the guard bed compared to the delay beds are due to more iodine being trapped in a smaller volume of bed than what was simulated for the delay beds. So, the bed power per volume for the guard bed is much higher in comparison with the larger delay beds. This higher power per volume is expected to cause higher temperatures. However, expected temperatures are not high enough to adversely affect the activated carbon chemically but would mitigate the delay time the guard bed achieves. Figure A.2 shows the distribution of ^{131}I in the simulated guard bed after 240 days of simulation.

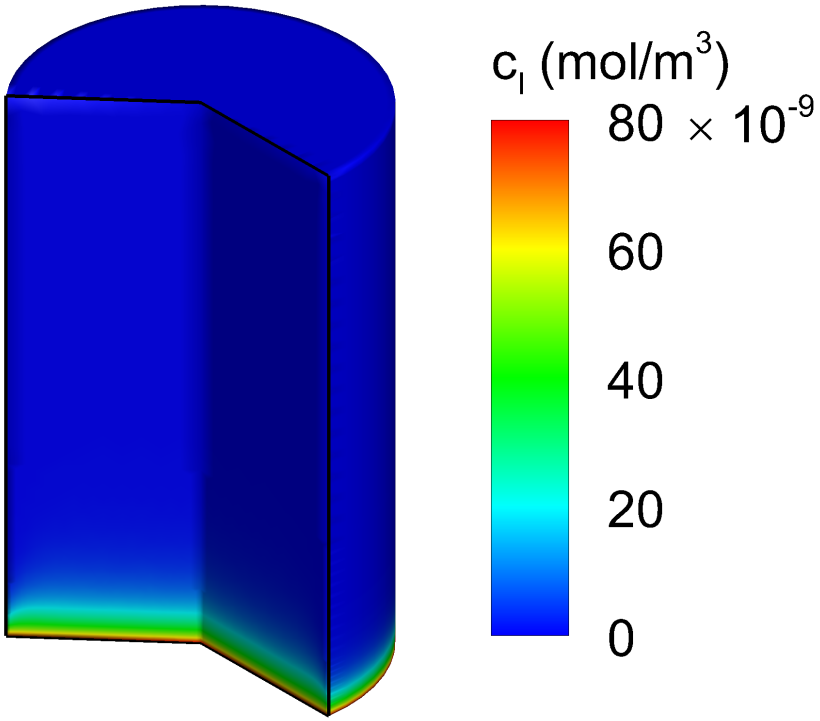

Figure A.2. Concentration distribution of ^{131}I (mol/m^3) after 240 days of simulation for the guard bed.

Despite the higher bed temperature, the simulated delay time of the guard beds is 228 days. Given that the longest-lived iodine species simulated was ^{131}I with an eight-day half-life, a 228-day delay time would eliminate most of the iodine. Ideal estimates of the iodine delay time at a constant temperature is 116 days. The fact that the model simulations, with higher average temperatures, have a longer delay time than an ideal calculation indicate that the finite element simulation needs increased meshing to produce a more accurate result. However, using the average temperature simulated by the finite element simulations (32°C) with ideal calculations, it is estimated that the guard bed delay time would be approximately 96 days. This is a 20 day decrease in guard bed performance compared to the model, but overall delay time should still be more than sufficient for the majority of the radioiodine heating to be captured.

A.2 Potential Pressure Loss

Modeling assumed the same flow of 16 scfm through the guard bed. While the delay beds have a larger bed diameter (90 in.), and hence a low pressure drop, the guard bed has a smaller diameter (10 in.). Preliminary calculations were performed to estimate the possible pressure loss through the guard bed.

The permeability of the activated coconut shell carbon (*k)* was estimated using the empirical equation developed by Rumpf and Gupte. [4] An estimation of the pressure drop was calculated using Darcy's law as shown in Equation 9 where *Q* is the volumetric flow, *A* is the area of the bed, μ is the viscosity of the fluid.

$$\frac{\Delta p}{L} = -\frac{Q\mu}{kA} \tag{9}$$

The estimated pressure losses due to the guard bed was estimated at 0.0079 psi using the porosity and particle diameters in Table 5.1. It is likely that such a low-pressure drop would not cause design issues. The estimated pressure drop with this same model through all delay beds is 0.0058 psi, which is similar to the proposed guard bed's pressure drop.

A.3 Conclusion

It is expected that the delay time, provided by the proposed guard bed, would remove most of the radioiodine heat from reaching the delay beds. Due to some heating of the guard bed occurring, it is recommended that a medical isotope producer integrate temperature monitoring of the guard bed outlet into their process. The temperature of the guard bed outlet can further refine estimates of how much radioiodine is reaching the guard bed, versus how much was held up in other prior process steps. The temperature of the guard bed outlet can be monitored by a thermocouple that is exposed to the abatement gas stream.

Pacific Northwest National Laboratory

902 Battelle Boulevard
P.O. Box 999
Richland, WA 99354
1-888-375-PNNL (7665)

www.pnnl.gov